Neuropharmacology 212 (2022) 109047

Contents lists available at ScienceDirect

Neuropharmacology

journal homepage: www.elsevier.com/locate/neuropharm

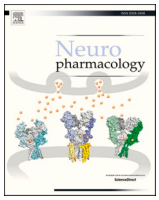

Homo-AMPA in the periaqueductal grey modulates pain and rostral ventromedial medulla activity in diabetic neuropathic mice

Enza Palazzo [a,*], Serena Boccella [a], Ida Marabese [a], Michela Perrone [a], Carmela Belardo [a], Monica Iannotta [a], Damiana Scuteri [b], Emanuela De Dominicis [a], Martina Pagano [a], Rosmara Infantino [a], Giacinto Bagetta [b], Sabatino Maione [a,c]

[a] Department of Experimental Medicine, Pharmacology Division, University of Campania "L. Vanvitelli", Naples, Italy
[b] Pharmacotechnology Documentation and Transfer Unit, Preclinical and Translational Pharmacology, Department of Pharmacy, Health and Nutritional Sciences, University of Calabria, Rende, Italy
[c] IRCSS, Neuromed, Pozzilli, Italy

ARTICLE INFO

Keywords:
Homo-AMPA
Diabetic neuropathic pain
Periaqueductal grey
Rostral ventromedial medulla
ON and OFF cells
mGluR6

ABSTRACT

The 2-amino-4-(3-hydroxy-5-methylisoxazol-4-yl)-butyric acid, homo-AMPA, an analog of α-amino-3-hydroxy-5-methyl-4-isoxazolepropionic acid (AMPA) and 2-aminoadipic acid, has shown no activity towards ionotropic and metabotropic glutamate 1, 2, 3, 4, 5, and 7 receptors (mGluR1-7), agonist activity at mGluR6 while the activity at mGluR8 was never investigated. The effect of homo-AMPA on pain control has been never investigated. In this study we evaluated the effect of intra-ventrolateral periaqueductal grey (VL PAG) microinjections of homo-AMPA on pain responses and the activity of pain-responding neurons of the rostral ventromedial medulla (RVM), the "pronociceptive" ON cells, and the "antinociceptive" OFF cells. The study was performed in control and diabetic neuropathic mice. Homo-AMPA decreased mechanical allodynia in diabetic neuropathic mice. Homo-AMPA increased also the latency to tail-flick, decreased the ongoing activity, the pain stimulus-evoked burst of firing, and the duration of the burst of the ON cells in both, control and neuropathic mice. Homo-AMPA also increased the ongoing activity, decreased and delayed the pause of the OFF cells in control mice. Unlike the retina, we did not find the transcript and protein for mGluR6 in the VL PAG. Alpha-methyl-serine-O-phosphate, a group III mGluRs antagonist, blocked the anti-allodynic effect of homo-AMPA. Considering the absence of both, mGluR6 in VL-PAG and homo-AMPA activity at mGluR4 and mGluR7 at the dose used, mGluR8 could be the target on which homo-AMPA produces the observed effects. The target of homo-AMPA capable of evoking analgesia at a very low dose and in conditions of diabetic neuropathy deserves further consideration.

1. Introduction

The 2-amino-4-(3-hydroxy-5-methylisoxazol-4-yl)-butyric acid, homo-AMPA, was developed as an analog of 2-aminoadipic acid, a glutamate homolog with a backbone extension, with the replacement of the distal carboxylic acid group with the bioisostere 3-hydroxyisoxazole. The 2-aminoadipic acid shows increased selectivity towards metabotropic glutamate receptors (mGluRs)(Bräuner-Osborne et al., 1996), the replacement of distal carboxylic acid with 3-hydroxyisoxazole of the homo-AMPA further restricts the selectivity towards mGluR6. Homo-AMPA proved to be inactive at ionotropic glutamate receptors (iGluRs) and mGluR1, 2, 3,4, and 7 showing to be a selective and rather potent agonist at mGluR6 with activity only 4 fold weaker than (S)–Glu (Bräuner-Osborne et al., 1996, 2000; Ahmadian et al., 1997; Schoepp et al., 1999). It is also noteworthy that although homo-AMPA exhibits high homology towards α-amino-3-hydroxy-5-methyl-4-isoxazolep ropionic acid (AMPA) it has no activity at AMPA receptors while its activity at mGluR8 has never been reported. Homo-AMPA is the main tool for the pharmacological characterization of mGluR6. Compared to the other mGluRs of the III group mGluR6 shows a high sensitivity to glutamate, slow desensitization (Nakajima et al., 1993), and a restricted localization in the retina where it mediates the response to light/dark on the bipolar ON cells (Nawy and Jahr, 1990; Morgans et al., 2009; Koike et al., 2010). The expression of mGluR6 was also found on microglia

* Corresponding author. Department of Experimental Medicine, Pharmacology Division, University of Campania "L. Vanvitelli", via Costantinopoli 16, 80138, Naples, Italy.
E-mail address: enza.palazzo@unicampania.it (E. Palazzo).

https://doi.org/10.1016/j.neuropharm.2022.109047
Received 9 August 2021; Received in revised form 22 February 2022; Accepted 26 March 2022
Available online 29 March 2022
0028-3908/

(Faden et al., 1997; Taylor et al., 2003), bone marrow stromal cells (Foreman et al., 2005), prostate cancer cells (Pissimissis et al., 2009), melanocytes (Devi et al., 2013), keratinocytes (Zheng et al., 2016), lymphocytes B (Vardi et al., 2011), and on peripheral tissues such as corneal endothelium, testis (Marciniak et al., 2016), kidney, conjunctiva, eyelid, and lymph nodes (B lymphocytes) (Vardi et al., 2011). Much more controversial is the demonstration of the presence of the mGluR6 in the CNS and in particular it has been found in the hypothalamus (Ghosh et al., 1997), nodose ganglia, the nucleus of the solitary tract (Hoang and Hay, 2001; Young et al., 2008), hippocampus (Dammann et al., 2018), cortical areas, superior colliculus, axons of the corpus callosum, accessory olfactory bulb, and the non-neuronal cells of the subcommissural organ (Vardi et al., 2011; Palazzo et al., 2020). These data indicating a wider expression of mGluR6 are in agreement with the finding that the administration of the homo-AMPA in the hippocampus produced an anxiolytic-like effect in the conflict drinking test in rats (Pałucha et al., 2004). The effect of homo-AMPA on pain control has never been investigated. Periaqueductal grey (PAG) is the main area of the pain descending pathway which through projections to the rostral ventromedial medulla (RVM) inhibits the ascending nociceptive transmission at the level of the dorsal horn of the spinal cord (Fields and Basbaum, 1999; Fields et al., 2005; Heinricher et al., 2009). In the RVM pain-responding neurons are found: the ON and OFF cells, which are activated and inhibited by pain stimuli, respectively (Fields et al., 1991), offering an electrophysiological method for evaluating/predicting the analgesic (or pain facilitating) effect of a drug. We have thus aimed in the current study at profiling the effects of intra-PAG administration of homo-AMPA on the pain threshold and the activity of ON and OFF neurons of the RVM. Since group III mGluRs proved to be particularly effective in modulating pain under pathological conditions (Boccella et al., 2020; Marabese et al., 2018; Palazzo et al., 2008, 2011, 2013, 2015; Rossi et al., 2014) we have chosen to conduct the study in control and diabetic neuropathic mice.

2. Methods

2.1. Animals

Male C57BL/6J mice (Envigo, Italy) weighing 22–25 g were housed three per cage under controlled illumination (12 h light/dark cycle; light on 6:00 a.m.) and standard environmental conditions (ambient temperature 20–22 °C, humidity 55–60%) for at least 1 week before the commencement of experiments. Mice chow and tap water were available ad libitum. The experimental procedures were approved by the Animal Ethics Committee of the University of Campania "L. Vanvitelli" of Naples. Animal care complied with Italian (D.L. 116/92) and European Commission (O.J. of E.C. L358/1 18/12/86) regulations on the protection of laboratory animals. All efforts were made to reduce both animal numbers and suffering during the experiments.

2.2. Induction of diabetes

Diabetes was induced by two injections, in two consecutive days, of streptozotocin (STZ, 90 mg/kg, i.p.) (Chem Cruz Biochemicals) freshly dissolved in sterile 0.9% saline accordingly to the method described by Jolivalt et al. (2017). The development of diabetes was confirmed by measuring the glucose concentration 5 days after the second STZ injection (day 0). Glucose levels in blood obtained from the tail vein were assayed using ACCU-CHEK test strips (Roche Diagnostics Corporation, Indianapolis, IN, USA). Only mice with high levels of blood glucose (>250 mg/dL) were included in the diabetic groups. Age-matched vehicle- (0.9% NaCl, saline) injected mice were used as controls. Diabetic mice showed mechanical allodynia, as shown by an increased sensitivity to von Frey filaments (Jolivalt et al., 2017). Only diabetic mice with evident mechanical allodynia tested by Von Frey were included in the study. Electrophysiological and behavioral experiments were performed 21 days after the second injection of STZ or vehicle (day 0). Each group of mice was used for 1 treatment and 1 test only. Experimenters were blind to the treatments in each experiment.

2.3. Mechanical allodynia

Mechanical allodynia was measured by a series of calibrated von Frey filaments (Stoelting, Wood Dale, IL, USA), ranging from 0.02 to 2 gr. Diabetic neuropathic mice were placed in plastic cages with a wire-mesh floor approximately 1 h before testing to allow behavioral accommodation. The von Frey filaments were applied in ascending order to the mid-plantar surface of the hind paw through the mesh floor. If the use of the filament three times did not induce a reaction, the next filament with higher pressure was used. The time interval before the application of each filament was at least 5 s. Data were expressed as mean ± S.E.M. of the mechanical withdrawal threshold (MWT) in grams.

2.4. Surgical preparation for intra-PAG microinjections

Control and diabetic mice were anesthetized with pentobarbital (50 mg/kg, i.p.), and a 26-gauge, 8 mm-long stainless steel guide cannula was stereotaxically lowered until its tip was 1.0 mm above the VL PAG (AP: −4.7 mm and L: 0.5 mm from bregma, V: 1.78 mm below the dura) (Paxinos and Franklin, 1997). The cannula was anchored with dental cement to a stainless steel screw in the skull. We used a David Kopf stereotaxic apparatus (David Kopf Instruments, Tujunga, CA, USA) with the animal positioned on a homeothermic temperature control blanket (Harvard Apparatus Limited, Edenbridge, Kent). Intra-VL PAG administration was conducted with a stainless steel cannula connected by a polyethylene tube to an SGE 1-μl syringe, inserted through the guide cannula, and extended 1.0 mm beyond the tip of the guide cannula to reach the VL PAG. Vehicle (0.05% DMSO in ACSF), homo-AMPA (6 nmol) or homo-AMPA (6 nmol) in combination with alpha-methyl-serine-O-phosphate (MSOP, 25 nmol), a group III mGluRs antagonist (Thomas et al., 1996), were injected in a volume of 0.2 μl into the VL PAG for 60 s and the injection cannula gently removed 2 min later.

2.5. Tail-flick

The day after the guide cannula implantation, anesthesia was induced with pentobarbital (50 mg/kg, i.p.) and maintained with a continuous infusion of propofol (5–10 mg/kg/h, i.v.). A thermal stimulus was elicited by a radiant heat source of a tail-flick unit (Ugo Basile, Varese, Italy), focused on the mouse tail approximately 1 cm from the tip. The intensity of the radiant heat source was adjusted to 50 mW (corresponding to 50 mJ per sec) at the beginning of each experiment to elicit a constant tail-flick latency. Tail-flicks were elicited and tail-flick latencies were recorded every 5 min for at least 15 min before and 75 min after the drug or vehicle microinjection into the VL PAG. To prevent tissue damage, the cut-off time was set at 25 s.

2.6. Single-unit extracellular recordings in the RVM

Single unit extracellular recordings have been carried out in the RVM while microinjecting homo-AMPA or vehicle into the VL PAG in control and diabetic mice. We implanted the cannula in the ventrolateral subregion of the PAG because output neurons from the VL PAG project directly to RVM (Sandkühler and Gebhart, 1984; Moreau and Fields, 1986). A glass-insulated tungsten filament electrode (3–5 MW) (FHC Frederick Haer& Co., ME, USA) was lowered into the RVM using the stereotaxic coordinates (AP: −6.48 mm and L: 0.3–0.5 mm from bregma, and V: 4.5–6.0 mm below the dura) from the atlas of Paxinos and Franklin (1997). Pain-responding neurons were identified by the characteristic OFF cell pause and ON cell burst of activity evoked by the

noxious stimulus. In particular, neurons showing an abrupt acceleration of firing activity were identified as ON cells and neurons showing an abrupt cessation of firing activity just before the pain-evoked nocifensive reaction as OFF cells. Neurons showing no change in activity just before the nocifensive reaction were identified as neutral cells (Fields et al., 1983) and were not recorded in the current study. The recorded signals were amplified and displayed on both, analog and a digital storage oscilloscope to ensure that the unit under study was unambiguously discriminated throughout the experiment. Signals were sampled by a CED 1401 interface (Cambridge Electronic Design Ltd., UK) and analyzed by Spike2 window software (CED, version 4) to create peristimulus rate histograms online and to store and analyze digital records of single-unit activity offline. The configuration, shape, and height of the recorded action potentials were monitored and recorded continuously using Spike2 software for online and offline analyses. Once an ON or OFF cell was identified from its background activity, we optimized spike size before all treatments. This study only included neurons whose spike configuration remained constant and could clearly be discriminated from the background activity throughout the entire experiment. By doing so, we were able to determine the activity of a single neuron only. In each mouse, the activity of only a single neuron was recorded before and after vehicle or drug administration. The ongoing activity, the average of the firing rate (spikes/sec) for 50 s before the noxious stimulus (which was carried out every 5 min), and noxious stimulus-evoked activity, the peak height (spikes/sec) of the noxious stimulus-evoked burst and the duration of the ON cell burst (the time of the increase in the frequency rate, which was at least twofold higher than its baseline) were quantified for the ON cells, before and after the VL PAG microinjection of vehicle or homo-AMPA. In diabetic mice, we were able to detect and measure the ongoing and evoked activity of the ON cells only, while no cell identifiable as OFF was found. The ongoing and evoked activity of the OFF cells was also investigated in control mice. For each OFF neuron the ongoing activity, measured in the same way as described for ON cells (see above), and the noxious-evoked activity, the latency to the onset of the pause (time between the onset of noxious stimulus application and the last action potential) and the duration of the pause (the time elapsing between the pause onset and the first action potential following noxious stimulus) were quantified. At the end of the experiment, a volume of 200 nl of neutral red (0.1%) was injected into the VL PAG for 30 min before killing the mice with a lethal dose of urethane. Mice were then perfused intracardially with 20 ml phosphate buffer solution (PBS) followed by 20 ml of 10% formalin solution in PBS. The brains were removed and immersed in a saturated formalin solution for 2 days. After fixation, the microinjection and recording sites were identified. The injection sites were ascertained using two consecutive sections (40 μm), one stained with cresyl violet to identify the microinjection site within the VL PAG, and the other unstained to determine dye spreading. The recording site was marked with a 20 μA DC applied for 20 s immediately prior to the end of the electrophysiological recordings. Only the data from drug microinjection and diffusion sites located within the VL PAG and those from the recording sites in RVM were included in the results. In particular, out of a total of 88 microinjections of vehicle or homo-AMPA, 9 were accidently performed outside the VL PAG and excluded from the results (Fig. 1). No pain-responding neurons identified by the characteristic OFF cell pause and ON cell burst of activity evoked by the noxious stimulus were found when the electrode was accidently placed outside the RVM. Each mouse has been used for a single cell recording. Before recording ON and OFF cell ongoing and noxious stimulus-evoked activity we explored cell population in RVM to define any changes of ON and OFF cell proportion in control and diabetic neuropathic mice. This exploration to identify ON or OFF neurons did not exceed three neurons per mouse.

2.7. mRNA extraction and reverse transcriptase-PCR

Total RNA was isolated from VL PAG and retina by using the TRIzol RNA Isolation Reagents, according to manufacturer's instructions and quantified using the ND-8000 spectrophotometer (NanoDrop Technologies, Wilmington, DE, USA). Afterward, single-stranded cDNA was synthesized from total RNA samples by using the High-Capacity cDNA Reverse Transcription Kit. The expression of mGluR6 transcript was determined independently by quantitative real-time PCR (qRT-PCR), using SYBR Green PCR Master Mix (Applied Biosystems, Foster City, CA, USA), and primer pairs rat specific to mGluR6 and GAPDH were

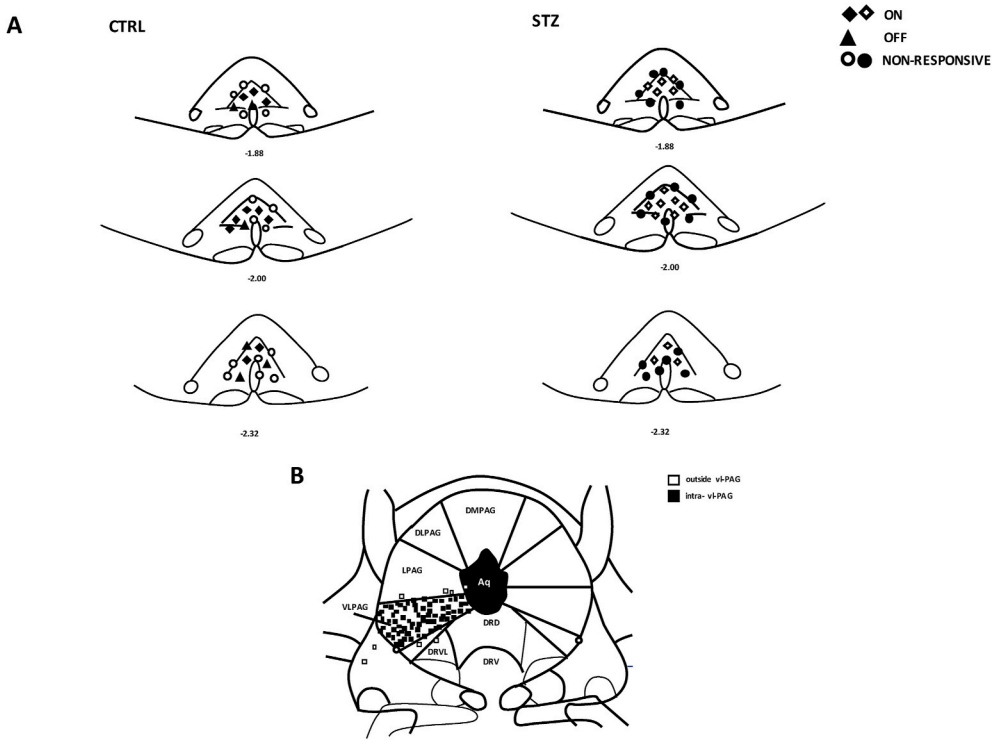

Fig. 1. Representative schematic illustration of the electrode locations within RVM (A) and microinjection sites for drug administration into the VL PAG (B). Coronal brain slices containing the VL PAG microinjection sites and RVM recording sites were processed after the experiments for histological analysis. The numbers under the illustration indicate the distance from the bregma (Paxinos and Franklin, 1997). Diamonds indicate ON cells and triangles OFF cells. The circles indicate neutral cells, non-responsive to pain stimulus. The black squares indicate microinjection sites, with overlapping symbols indicated once, within the VL PAG while the white squares indicated microinjection sites outside the VL PAG that were not considered in the data analysis.

purchased from Qiagen (Hilden, Germania). To normalize total RNA samples, glyceraldehyde-3-phosphate dehydrogenase (GAPDH) was selected as an appropriate constitutively expressed endogenous control gene.

2.8. Western blot

Each animal, previously anesthetized, was decapitated, the brain and **eyes** removed and dissected to collect the VL PAG and retinas, washed twice in cold PBS (without $Ca^{2+}$and Mg^{2+}, pH 7.4), and homogenized in protein lysis buffer [HEPES 25 mM; EDTA 5 mM; SDS 1%; Triton X-100 1%; PMSF 1 mM; $MgCl_2$ 5 mM; Protease Inhibitor Cocktail (Roche, Mannheim, Germany); Phospahatase Inhibitor Cocktail (Roche, Mannheim, Germany)]. Lysates were then centrifuged for 15 min at 13,000 g at 4 °C, and the supernatants were transferred into clear tubes, and quantified by DC Protein Assay, boiled for 5 min in Laemmli SDS loading buffer, loaded on 10–15% SDS-polyacrylamide gel electrophoresis, and then transferred to a PVDF membrane. Filters were incubated overnight at 4 °C with the rabbit antibody mGluR6 (1:1000, Mybiosource: MBS555139). Themonoclonal GAPDH (1:5000, Santa Cruz Biotechnology, Dallas, Texas) antibody was used to check for equal protein loading. Immunoreactive bands were visualized by using an enhanced chemiluminescence system (ThermoFisher, 35055), then quantified with VisionWorks Life Science Image Acquisition and Analysis software (UVP, Upland, CA, USA) and expressed as densitometric units (DU).

2.9. Drugs

Homo-AMPA and MSOP were purchased by Tocris Cookson Ltd., (Bristol). Homo-AMPA was dissolved in 0.05% dimethyl sulphoxide (DMSO) in artificial cerebrospinal fluid (ACSF, composition in mM: 125 NaCl, 2.5 KCl, 1.18 $MgCl_2$, and 1.26 $CaCl_2$) on the day of the experiment. MSOP was dissolved in ACSF. The drug solution was microinjected into the VL PAG in a volume of 0.2 μl. Control mice received the same volume of vehicle (0.05% DMSO in ACSF). The dose of 6 nmol for homo-AMPA was chosen to start from the EC50 value (Bräuner-Osborne et al., 1996; Ahmadian et al., 1997) and choosing the lowest dose (6 nmol corresponding to 30 μM) able to modify the pain threshold and the activity of the RVM neurons. The dose of MSOP was chosen based on previous studies in which the MSOP was microinjected into the VL PAG and showed no effect per se (Maione et al., 1998; Palazzo et al., 2001; Berrino et al., 2001; Marabese et al., 2007a,b).

2.10. Statistics

All data are expressed as mean ± SEM. Statistically significant differences between the different groups of mice have been analyzed by two-way analysis of variance (ANOVA) for repeated measures followed by Tukey's post hoc test. Two-way ANOVA for repeated measures followed by Sidak's post hoc test has been used to compare post-injection *vs* pre-injection values. $P < 0.05$ was considered statistically significant.

3. Results

3.1. Effect of intra-VL PAG homo-AMPA administration on paw withdrawal threshold in diabetic neuropathic mice

Mechanical allodynia was measured only in diabetic neuropathic mice 21 days after STZ administration (Fig. 2A). Mechanical withdrawal threshold (MWT) to von Frey filament stimulation was measured 15 min prior and for 120 min (every 15 min) after microinjecting vehicle, homo-AMPA (6 nmol), or homo-AMPA (6 nmol) in combination with MSOP (25 nmol) into the VL-PAG. Before STZ administration, the MWT was 1.875 ± 0.07, 1.92 ± 0.07, and 1.725 ± 0.19 g in groups of mice intended to receive STZ/vehicle, STZ/homo-AMPA, and STZ/homo-AMPA + MSOP, respectively. Diabetic neuropathic mice before vehicle (0.058 ± 0.008 g, $p < 0.0001$, $n = 8$), homo-AMPA (0.058 ± 0.008 g, $p < 0.0001$, $n = 8$) or homo-AMPA + MSOP (0.09 ± 0.02, $p < 0.0001$, $n = 8$) administration showed a decrease in the MWT (Fig. 2B). Intra-VL PAG microinjection of the vehicle did not change the MWT in diabetic neuropathic mice (0.10 ± 0.033 g, $p = 0.9973$ at 30 min post-administration, two-way ANOVA for repeated measures followed by Sidak's post hoc test) compared to pretreatment values (Fig. 2B). Intra-VL PAG microinjection of homo-AMPA increased the MWT in neuropathic mice with a peak of the effect at 30 min from drug-administration (1.8 ± 0.07 g, $p < 0.0001$, two-way ANOVA for repeated measures followed by

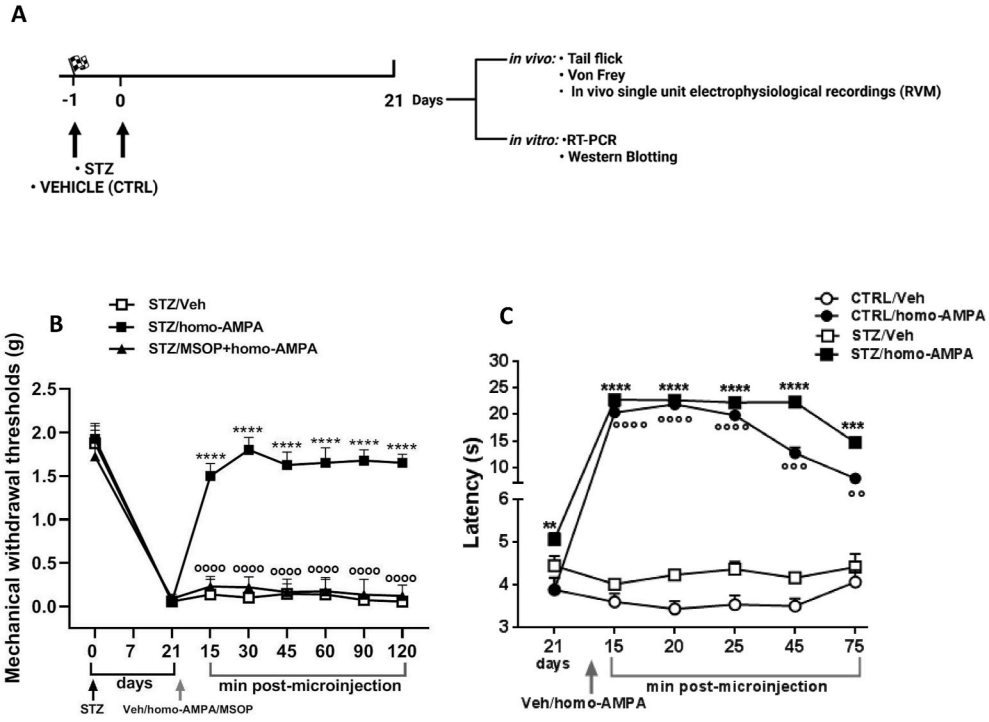

Fig. 2. Panel "A" shows the timeline for the induction of diabetes with 2 consecutive streptzotocin administration (or saline in the control group, CTRL) and the performance of the in vivo (tail-flick, von Frey, and single-unit electrophysiological recordings) and in vitro (RT PCR and western blot) experiments. Panel "B" shows the effects of a single intra-VL PAG microinjection of vehicle (veh, 0.05% DMSO in ACSF), homo-AMPA (6 nmol), or homo-AMPA (6 nmol) in combination with MSOP (25 nmol) on mechanical withdrawal threshold (MWT) in diabetic neuropathic mice (STZ) before and 21 days after the STZ administration. Panel "C" shows the effects of single intra-VL-PAG microinjection of homo-AMPA or the respective vehicle on tail-flick latencies in control (CTRL) and diabetic neuropathic mice (STZ). Each point represents the mean ± S.E.M of 8-6 mice per group. ° indicates statistically significant difference vs STZ/homo-AMPA (B) and vs CTRL/veh (C) while * indicates significant difference vs STZ/vehicle (B and C). P values < 0.05 were considered statistically significant. °° corresponds to $p < 0.01$, °°° and *** to $p < 0.001$, and °°°° and **** to $p < 0.0001$.

Tukey's post hoc test) compared to vehicle-treated neuropathic mice. The duration of the anti-allodynic effect of homo-AMPA in diabetic mice lasted until the end of the observation period (120 min post-drug) (Fig. 2B). The intra-VL PAG administration of MSOP (25 nmol), a group III mGluRs antagonist, in combination with homo-AMPA (6 nmol) antagonized the effect of the latter (0.22 ± 0.6 g, $p < 0.0001$, at 30 min post-administration, two-way ANOVA for repeated measures followed by Tukey's post hoc test) compared to homo-AMPA-microinjected neuropathic mice (Fig. 2B). Two-way ANOVA for repeated measures showed a significant effect of treatments ($F_{2,9} = 185.5$, $p < 0.0001$), time ($F_{7,63} = 213.7$, $p < 0.0001$), and a significant interaction of time x treatment ($F_{14,63} = 45.16$, $p < 0.0001$).

3.2. Effect of intra-VL PAG microinjection of homo-AMPA on tail-flick latencies in control and diabetic neuropathic mice

Tail-flicks were elicited every 5 min for 15 min before and for 60 min after microinjection of the homo-AMPA or respective vehicle into the VL-PAG. In control mice, tail-flick latency was 3.88 ± 0.28 s (n = 6). The microinjection of the vehicle into the VL PAG did not change tail-flick latency in control mice (3.43 ± 0.184 s, $p = 0.7742$, at 20 min post-administration, two-way ANOVA for repeated measures followed by Sidak's post hoc test) compared to pretreatment values. The microinjection of homo-AMPA (6 nmol) in control mice increased the tail-flick latency with a peak of the effect 20 min after drug administration (21.85 ± 0.54 s, $p < 0.0001$, two-way ANOVA for repeated measures followed by Tukey's post hoc test) compared to vehicle-microinjected mice. In diabetic neuropathic mice tail-flick latency was 5.06 ± 0.15 s (n = 6). Intra-VL PAG microinjection of the vehicle did not change the tail-flick latency in diabetic neuropathic mice (4.233 ± 0.117 s, $p = 0.9634$, at 20 min post-administration, two-way ANOVA followed by Sidak's post hoc test) compared to pretreatment values (Fig. 2C) while the microinjection of homo-AMPA into the VL PAG increased the tail-flick latency to 22.6 ± 0.83 s ($p < 0.0001$, two-way ANOVA for repeated measures followed by Tukey's post hoc test) at 20 min post-administration, compared to vehicle-microinjected neuropathic mice (Fig. 2C). Two-way ANOVA for repeated measures showed a significant effect of treatments ($F_{3,20} = 650.7$, $p < 0.0001$), time ($F_{5,100} = 216.2$, $p < 0.0001$), and a significant interaction of time x treatment ($F_{15,100} = 88.18$, $p < 0.0001$).

3.3. Percentage of ON and OFF cells in the RVM in control and neuropathic mice

We first investigated the percentage of ON (responding with an excitation, the ON cell burst, to the noxious stimulus) and OFF (responding with an inhibition, the OFF cell pause, to the noxious stimulus) neurons in the RVM in control and diabetic neuropathic mice. In control mice, out of a total of 31 neurons encountered 32.26% were classified as ON cells (n = 10) and 19.35% as OFF cells (n = 6), while the rest, 48.39% of the encountered cells (n = 15), did not respond to noxious stimulation (likely neutral, serotoninergic, or unidentified cells, Gao and Mason, 2000). In neuropathic mice, out of a total of 33 neurons encountered 45.45% were classified as ON cells (n = 15) and the remaining 54.54% of the encountered neurons (n = 18) did not respond to the noxious stimulation. Ultimately, in neuropathic mice OFF cells

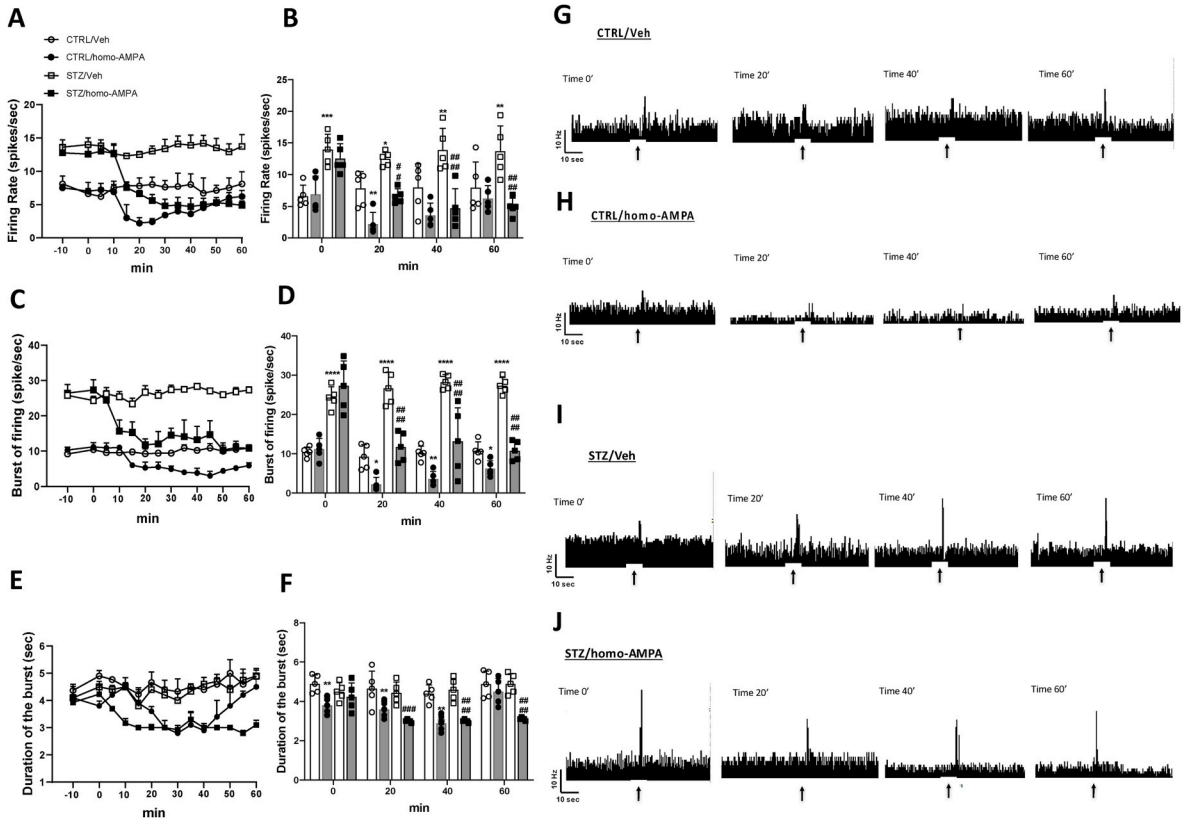

Fig. 3. Effects of intra-VL PAG microinjection of homo-AMPA (6 nmol, 0.2 μl) or respective vehicle (veh, 0.05% DMSO in ACSF, 0.2 μl) on the ON cell activity in control (CTRL) and diabetic neuropathic (STZ) mice. Panels "A" and "B" show the spontaneous firing rate, "C" and "D" the burst of firing, and "E" and "F" the duration of the burst of the ON cells in control and diabetic neuropathic mice before and after the intra-VL PAG administration of homo-AMPA or respective vehicle. Panels "G", "H", "I", and "J" show examples of ratemater records illustrating the effect of intra-VL PAG microinjection of vehicle (G and I) or homo-AMPA (H and J) on either the firing rate or burst of the firing of identified RVM ON cells in control (G and H) and diabetic neuropathic mice (H and J). Each point represents the mean ± S.E.M. * indicates statistically significant difference vs CTRL/veh and $^{\#}$vs STZ/vehicle. P values < 0.05 were considered statistically significant. * corresponds to $p < 0.05$, ** and $^{\#\#}$ to $p < 0.01$, *** and $^{\#\#\#}$ to $p < 0.001$, and **** and $^{\#\#\#\#}$ to $p < 0.0001$.

were not found.

3.4. Effects of intra-VL PAG microinjection of homo-AMPA on the ongoing and evoked activity of ON and OFF cells in control mice

In control mice, the population of the ON cells had a firing rate of the spontaneous activity of 6.6 ± 0.8 spikes/sec (Fig. 3A and B), a burst of the firing of 10.44 ± 0.55 spikes/sec (Fig. 3C and D) and a duration of the burst of 4.9 ± 0.20 s, n = 5 (Fig. 3E and F). The microinjection of the vehicle did not change the firing rate (7.8 ± 1.2 spikes/sec, p = 0.9471, at 20 min post-administration, two-way ANOVA for repeated measures followed by Sidak's post hoc test) (Fig. 3A and B), the burst of firing (9.26 ± 1.37 spikes/sec, p = 0.9320, at 20 min post-administration, two-way ANOVA for repeated measures followed by Sidak's post hoc test) (Fig. 3C and D), and the duration of the burst (4.66 ± 0.39 s, p = 0.9802, at 20 min post-administration, two-way ANOVA for repeated measures followed by Sidak's post hoc test) (Fig. 3E and F) of the ON cells compared to pretreatment values. The intra-VL PAG microinjection of homo-AMPA (6 nmol) decreased the firing rate of the ON cells (2.20 ± 0.80 spikes/sec, p = 0.0063, at 20 min post-administration, two-way ANOVA for repeated measures followed by Tukey's post hoc test) (Fig. 3A and B) compared to vehicle-treated mice (Table 1A). Homo-AMPA also decreased the ON cell burst of firing (5.30 ± 1.60 spike/sec, p = 0.032, at 20 min post-administration, two-way ANOVA for repeated measures followed by Tukey's post hoc test)(Fig. 3C and D, and Table 1B), and the duration of the burst (3.60 ± 0.18 s, p = 0.0081, at 20 min post-administration, two-way ANOVA for repeated measures followed by Tukey's post hoc test) compared to vehicle-treated mice (Fig. 3E and F, and Table 1C). In control mice, the population of OFF cells had a spontaneous firing rate of 8.3 ± 1.2 spikes/sec and duration of pause of 4.2 ± 0.5 s (Fig. 4A–D). Microinjection of vehicle did not change the firing rate (8.4 ± 0.90 spikes/sec, p > 0.999, at 20 min post-administration, two-way ANOVA for repeated measures followed by Sidak's post hoc test) and the duration of the pause (4.3 ± 0.70 s, p > 0.99, at 20 min post-administration, two-way ANOVA for repeated measures followed by Sidak's post hoc test) of the OFF cells compared to pretreatment values (Fig. 4A–D). The intra-VL PAG microinjection of homo-AMPA (6 nmol) increased the firing rate of the OFF cells (11 ± 0.12 spikes/sec, p = 0.047, at 20 min post-administration, two-way ANOVA for repeated measures followed by Sidak's post hoc test)(Fig. 4A and B, and Table 2A) compared to vehicle-treated mice. Homo-AMPA also decreases the duration of the OFF cell pause (3.0 ± 0.9 s, p = 0.47, at 20 min post-administration, two-way ANOVA for repeated measures followed by Sidak's post hoc test) compared to vehicle-treated mice (Fig. 4C and D, and Table 2B). The E and F panels of Fig. 4 are examples of ratemater records illustrating the effect of intra-VL PAG microinjection of vehicle (Fig. 4E) or homo-AMPA (Fig. 4F) on either the firing rate or duration and onset of the pause of identified RVM OFF cells in control mice.

3.5. Effects of intra-VL PAG microinjection of homo-AMPA on the ongoing and evoked activity of ON cells in diabetic neuropathic mice

In diabetic mice, the population of ON cells had an ongoing firing rate of 14 ± 1.1 spikes/sec (Fig. 3A and B), and a burst of the firing of 24.30 ± 1.2 spikes/sec that were higher compared to control mice (p = 0.0002, and p < 0.0001, respectively, two-way ANOVA for repeated measures followed by Tukey's post hoc test) (Fig. 3C and D). Instead, the duration of burst in diabetic mice did not change (4.5 ± 0.2 s, p = 0.6, two-way ANOVA for repeated measures followed by Tukey's post hoc test) compared to the control mice (Fig. 3E and F). Microinjection of the vehicle did not change the firing rate (12.5 ± 0.5 spikes/sec, p = 0.744, at 20 min post-administration, two-way ANOVA for repeated measures followed by Sidak's post hoc test) (Fig. 3A and B), the burst of firing (26.7 ± 1.80 Hz, p = 0.7318, at 20 min post-administration, two-way ANOVA for repeated measures followed by Sidak's post hoc test) (Fig. 3C and D), and the duration of the burst (4.4 ± 0.24 s, p = 0.9969, at 20 min post-administration, two-way ANOVA for repeated measures followed by Sidak's post hoc test) (Fig. 3E and F) of the ON cells compared to pretreatment values.

Intra-VL PAG microinjection of homo-AMPA caused a decrease in the firing rate (6.6 ± 0.5 spikes/sec, p < 0.0001, at 20 min post-administration, two-way ANOVA for repeated measures followed by

Table 1
Statistically significant differences found comparing the ongoing firing rate (A), burst of firing (B) and duration of the burst (C) of the ON cells in control (CTRL) and diabetic neuropathic (STZ) mice treated with vehicle or with homo-AMPA. Two-way ANOVA for repeated measures followed by Tukey's post-hoc test was used for calculating the statistical significance. Each point represents the mean ± S.E.M. * indicates statistically significant difference vs CTRL/veh, ° vs STZ/vehicle and # vs CTRL/homo-AMPA. P values < 0.05 were considered statistically significant.

A	CTRL/Homo AMPA vs. CTRL/Veh	STZ/Veh vs. CTRL/Veh	STZ/Veh vs. CTRL/Homo AMPA	STZ/Homo AMPA vs. CTRL/Homo AMPA	STZ/Homo AMPA vs. STZ/Homo AMPA
-10	ns	**	##	##	ns
0	ns	****	###	##	ns
5	ns	****	###	##	ns
10	ns	**	##	##	ns
15	*	*	####	#	°
20	**	*	####	#	°°
25	**	*	####	ns	°°°°
30	*	**	####	ns	°°°°
35	ns	***	####	ns	°°°°
40	*	**	####	ns	°°°°
45	ns	****	####	ns	°°°°
50	ns	***	####	ns	°°°°
55	ns	**	###	ns	°°°°
60	ns	**	####	ns	°°°°
B	CTRL/Homo AMPA vs. CTRL/Veh	STZ/Veh vs. CTRL/Veh	STZ/Veh vs. CTRL/Homo AMPA	STZ/Homo AMPA vs. CTRL/Homo AMPA	STZ/Homo AMPA vs. STZ/Homo AMPA
-10	ns	**	##	##	ns
0	ns	****	###	##	ns
5	ns	****	###	##	ns
10	ns	**	##	##	ns
15	*	*	####	#	°
20	**	*	####	#	°°
25	**	*	####	ns	°°°°
30	*	**	####	ns	°°°°
35	ns	***	####	ns	°°°°
40	*	**	####	ns	°°°°
45	ns	****	####	ns	°°°°
50	ns	***	####	ns	°°°°
55	ns	**	###	ns	°°°°
60	ns	**	####	ns	°°°°
C	CTRL/Homo AMPA vs. CTRL/Veh	STZ/Veh vs. CTRL/Veh	STZ/Veh vs. CTRL/Homo AMPA	STZ/Homo AMPA vs. CTRL/Homo AMPA	STZ/Homo AMPA vs. STZ/Homo AMPA
-10	ns	**	##	##	ns
0	ns	****	###	##	ns
5	ns	****	###	##	ns
10	ns	**	##	##	ns
15	*	*	####	#	°
20	**	*	####	#	°°
25	**	*	####	ns	°°°°
30	*	**	####	ns	°°°°
35	ns	***	####	ns	°°°°
40	*	**	####	ns	°°°°
45	ns	****	####	ns	°°°°
50	ns	***	####	ns	°°°°
55	ns	**	###	ns	°°°°
60	ns	**	####	ns	°°°°

*,°,# P < 0.05, **,°°, ## P < 0.01, ***,°°°, ###P < 0.001 and ****,°°°°, ####P < 0.0001.

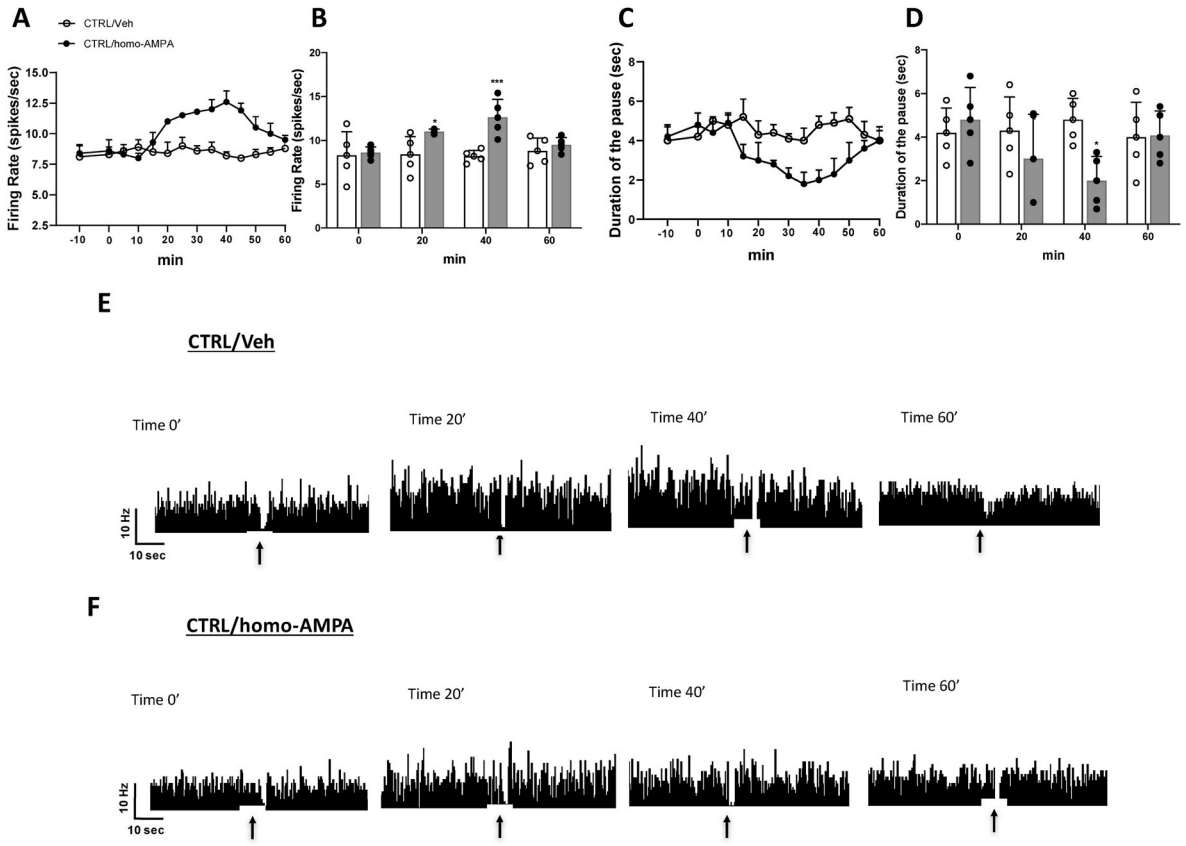

Fig. 4. Effects of intra-VL PAG microinjection of homo-AMPA (6 nmol, 0.2 μl) or respective vehicle (0.05% DMSO in ACSF, 0.2 μl) on the OFF cell activity in control mice. Panels "A" and "B" show the spontaneous firing rate and "C" and "D" the duration of the pause in control mice before and after the intra-VL PAG administration of homo-AMPA or respective vehicle. Panels "E" and "F" show examples of ratemater records illustrating the effect of intra-VL PAG microinjection of vehicle (E) or homo-AMPA (F) on either the firing rate or duration of the pause of identified RVM OFF cells in control mice. Each point represents the mean ± S.E.M. * indicates statistically significant difference vs CTRL/veh. P values < 0.05 were considered statistically significant. * corresponds to $p < 0.05$ and *** to $p < 0.001$.

Sidak's post hoc test)(Fig. 3A and B), the burst of firing (11.77 ± 1.68 spikes/sec, $p < 0.0001$, at 20 min post-administration, two-way ANOVA for repeated measures followed by Sidak's post hoc test) (Fig. 3C and D), and duration of the burst (3 ± 0.12 s, $p < 0.0001$, at 20 min post-administration, two-way ANOVA for repeated measures followed by Sidak's post hoc test) (Fig. 3E and F) of the ON cells compared to pre-treatment values. The effect of homo-AMPA on the ongoing activity and burst of firing on the ON cells in diabetic mice was higher compared to control mice ($p = 0.046$ and 0.033, respectively, at 20 min post-administration, two-way ANOVA for repeated measures followed by Tukey's post hoc test) (Fig. 3A–D and Table 1). However, the duration of the burst after the administration of homo-AMPA did not differ in diabetic neuropathic mice compared to control mice ($p = 0.24$, at 20 min post-administration, two-way ANOVA for repeated measures followed by Tukey's post hoc test). The J-I panels of Fig. 3 are examples of ratemater records illustrating the effect of intra-VL PAG microinjection of vehicle (Fig. 3G and I) or homo-AMPA (Fig. 3H and J) on either the firing rate or burst of the firing of identified RVM ON cells in control (Fig. 3G and H) and diabetic neuropathic mice (Fig. 3H and J).

3.6. Expression of mGluR6 transcripts in the VL PAG and retinas

qRT-PCR analysis did not detect the presence of mGluR6 within the VL PAG either in control mice (n = 3) **or** in diabetic neuropathic mice (n = 3). Otherwise, the mGluR6 was present in the retina of both, control (n = 3) and neuropathic diabetic mice (n = 3) with a reduction of about 40% in diabetic neuropathic mice compared to control mice (Fig. 5A).

3.7. Expression of mGluR6 protein in the VL PAG

Western blot did not detect the presence of mGluR6 protein within the VL PAG either in control mice (n = 3) than in diabetic neuropathic mice (n = 3). Otherwise, the mGluR6 protein was found in the retina of both, control (n = 3) and neuropathic diabetic mice (n = 3) with a reduction of the levels of expression in diabetic neuropathic mice compared to control mice (Fig. 5B).

4. Discussion

4.1. The microinjection of homo-AMPA in the VL-PAG produces analgesia and consistently modulates the activity of RVM in control mice

A prerogative for the characterization of the pathophysiological role and pharmacological relevance of glutamate receptor subtypes is the availability of highly selective ligands. Regarding metabotropic glutamate receptors, which are the most suitable substrate to modulate glutamate neurotransmission which is often dysregulated in various neurological and psychiatric disorders, highly selective ligands for each receptor subtype ($mGluR_{1\text{-}8}$) are available today (O'Brien and Conn, 2016). Homo-AMPA has been developed and described as a selective agonist at mGluR6 (EC50 = 58 ± 11 μM), ineffective at ionotropic glutamate receptors (iGluRs) and mGluR1, 2, 3, 4, 5, and 7 despite the isomer R, (R)-homo-AMPA, showed a weak antagonist activity at N-methyl-D-aspartic acid (NMDA) receptor (IC50 = 131 ± 18 μM). The selectivity of homo-AMPA on mGluR8 has never been investigated so far (Bräuner-Osborne et al., 1996, 2000; Ahmadian et al., 1997). As there are no other selective ligands for mGluR6, homo-AMPA has become the

Table 2
Statistically significant differences found comparing the ongoing firing rate (A), and duration of the pause **(B)** of the OFF cells in control (CTRL) mice treated with vehicle or with homo-AMPA. Two-way ANOVA for repeated measures followed by Tukey's post-hoc test was used for calculating the statistical significance. Each point represents the mean ± S.E.M. * indicates statistically significant difference vs CTRL/veh. P values < 0.05 were considered statistically significant.

A	CTRL/HOMO AMPA vs. CTRL/Veh
−10	ns
0	ns
5	ns
10	ns
15	ns
20	ns
25	ns
30	**
35	**
40	****
45	***
50	ns
55	ns
60	ns
B	CTRL/HOMO AMPA vs. CTRL/Veh
−10	ns
0	ns
5	ns
10	ns
15	ns
20	ns
25	ns
30	ns
35	ns
40	*
45	*
50	ns
55	ns
60	ns

*P < 0.05, **P < 0.01, ***P < 0.001 and ****P < 0.0001.

gold standard compound for characterizing the role of this receptor. There is an urgent need for effective and well-tolerated drugs against chronic pain and studies focused on the role of group III mGluRs have so far been addressed at receptor subtypes 4, 7, and 8 (Vilar et al., 2013; Wang et al., 2011; Maione et al., 1998, 2000; Berrino et al., 2001; Palazzo et al., 2001, 2008, 2011, 2013, 2015; Marabese et al., 2007 a,b) excluding mGluR6 although different evidence showed broader receptor expression rather than tight confinement in the retina (Vardi et al., 2011; Palazzo et al., 2020). Among the brain areas controlling pain, the PAG plays a relevant role as it represents the main area of the descending pathway of pain (Fields et al., 2005; Heinricher et al., 2009). PAG-induced analgesia is mainly produced through the modulation of neurons within the RVM (Behbehani and Fields, 1979; Prieto et al., 1983) whose projections to the spinal dorsal horn inhibit the activity of nociceptive neurons and pain responses (Fields et al., 1999; Salas et al., 2016). Two populations of pain-responding neurons are found within the RVM: the ON cells, defined as "pronociceptive" since they are excited by nociceptive stimuli and inhibited by analgesics such as morphine, and the OFF cells, defined as "antinociceptive" since they are inhibited by nociceptive stimuli and activated by morphine (Fields et al., 1991).

In this study, we injected homo-AMPA into the VL PAG and monitored pain responses and the activity of the ON and OFF cells of the RVM. Since group III mGluRs show activity specially in conditions of pathological pain (Boccella et al., 2020; Marabese et al., 2018; Palazzo et al., 2008, 2011, 2013, 2015; Rossi et al., 2014) we decided to conduct the study on control and neuropathic diabetic mice, also in consideration of the fact that diabetes is associated with retinopathy and the mGluR6 receptor is been highly characterized in the retina.

The microinjection of homo-AMPA into the VL PAG increased the tail-flick latency, inhibited the activity of the ON cells, and enhanced that of the OFF cells in control mice. In particular, the intra-VL PAG microinjection of homo-AMPA decreased the ongoing activity, the evoked frequency of the burst, and the duration of the burst of the ON cells. It also increased the ongoing activity and the evoked onset of the pause while decreasing the duration of the pause of the OFF cells in control mice. These effects correspond to an enhancement of the descending inhibition of pain and are consistent with the behavioral analgesia observed in the tail-flick.

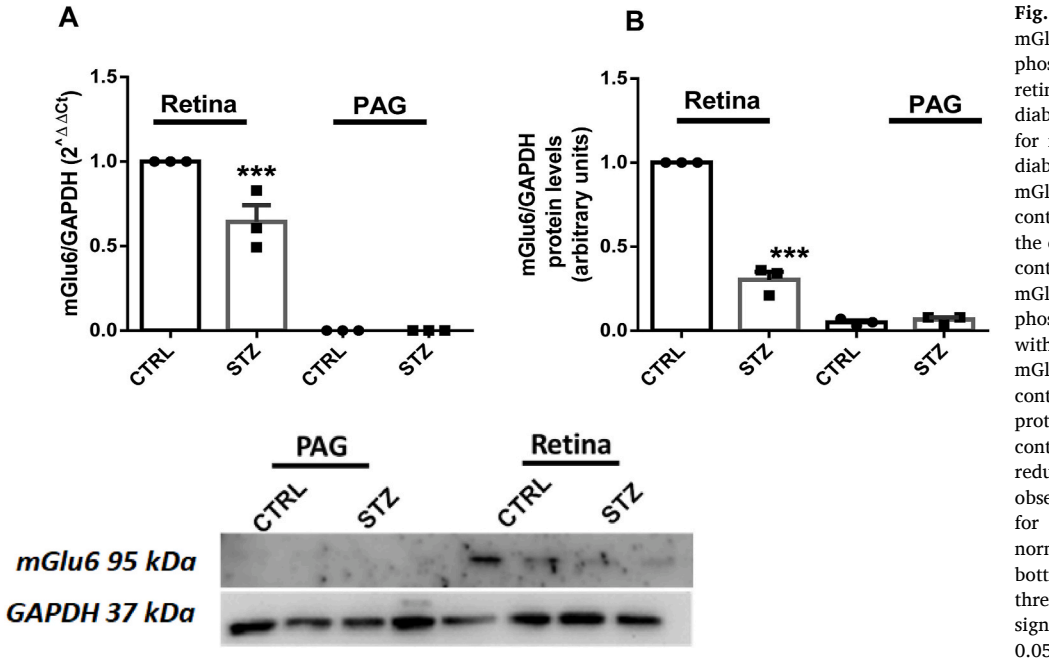

Fig. 5. "A" shows the mRNA levels of mGluR6 normalized to glyceraldehyde 3-phosphate dehydrogenase (GADPH) in the retina and VL PAG of control (CTRL) and diabetic mice (STZ). We found no transcripts for mGluR6 in the VL PAG of control and diabetic mice. Otherwise, the mRNA for mGluR6 was present in the retina of both, control and diabetic mice with a reduction of the expression in diabetic mice compared to control mice. "B" shows the protein levels of mGluR6 normalized to glyceraldehyde 3-phosphate dehydrogenase (GADPH). As with the transcripts, we did not find the mGluR6 protein in the VL PAG of both, control and diabetic mice. The mGluR6 protein was present in the retina of both control and diabetic mice. In diabetic mice, a reduction in mGluR6 protein levels was observed. A representative gel blot analysis for mGluR6 protein (western blotting) normalized vs GADPH is also shown in the bottom. Data represent the mean ± S.E.M of three mice per group. * indicates statistically significant difference vs CTRL. P values < 0.05 were considered statistically significant.

4.2. The microinjection of homo-AMPA in the VL PAG reduces mechanical allodynia and consistently modifies RVM neural activity in diabetic neuropathic mice

Mice receiving STZ showed increased blood glucose levels. Peripheral neuropathy is a frequent complication of chronic diabetes and mechanical allodynia is a painful manifestation of neuropathy in both, humans (Vinik et al., 1995; Bastyr et al., 2005) and rodents (Morrow, 2004; Lee-Kubli et al., 2014). In particular, diabetic rodents develop increased sensitivity to a series of manual von Frey filaments within 2–4 weeks from the induction of diabetes (Calcutt et al., 1996). Consistently, we found mechanical allodynia 21 days after the induction of diabetes by STZ. Furthermore, we found changes in the percentage and activity of ON and OFF cells in diabetic neuropathic mice with an increase in the number of the ON cells and an enhancement of their activity.

The RVM is the connecting area between the PAG, which in turn collects inputs from the amygdala, hypothalamus and cortex, and the dorsal horns of the spinal cord. In chronic pain conditions an imbalance in the neural activity of the RVM with a clear activation of the ON cells and inactivation of the OFF cells is widely reported (Millan, 2002; Vanegas and Schaible, 2004; Heinricher et al., 2009; Ossipov et al., 2010; Khasabov et al., 2012; Silva et al., 2013; Palazzo et al., 2013; Rossi et al., 2014; Marabese et al., 2018). The hyperactivity of the ON cells accounts for an enhancement of the descending facilitation while the depression of the OFF cells accounts for a reduction of the descending inhibition causing overall hyperactivity of the spinal neurons and exacerbation of pain (Millan, 2002; Vanegas and Schaible, 2004; Heinricher et al., 2009; Ossipov et al., 2010; Khasabov et al., 2012; Silva et al., 2013; Palazzo et al., 2013; Rossi et al., 2014; Marabese et al., 2018). Similarly, enhancement of the ON cell activity concomitantly with inhibition of the OFF cells was also found in STZ-induced diabetic neuropathic pain in a previous (Silva et al., 2013) and the current study. In particular, we found an increase in the number, spontaneous, and evoked activity of ON cells concomitantly with an apparent absence of active OFF cells on the total of pain-responding cells encountered in the RVM. Thus the prevalence of pain facilitation over pain inhibition from the RVM may account for the pain exacerbation also in diabetic neuropathic pain.

Although a reduction in the number of active OFF cells was already observed in neuropathic pain (Leong et al., 2011) and diabetic neuropathy (Silva et al., 2013), in the present study the effect on OFF cells was more dramatic. In fact, while in the aforementioned studies a reduction in the number of OFF cells was observed, in our study we observed the complete silencing of OFF cells. Regarding the study conducted on the same diabetic neuropathy model, the different species used (mouse versus rat), the length of time elapsed from the administration of STZ (3 versus 4 weeks) and the number of cells that were analyzed (33 versus 56 neurons) can explain the observed differences. Regarding the mechanisms responsible for this neuronal shutdown of OFF cells, the neuron death hypothesized in the neuropathic pain model (Leong et al., 2011) cannot be confirmed in the diabetic neuropathic pain model (Silva et al., 2013 and the current study) and it could plausibly depend on the increased activity (and number) of GABA-containing ON cells (Fields et al., 1991) since an increase in GABAergic inhibition following diabetic neuropathy has been demonstrated in the spinal cord (Morgado et al., 2008).

The intra-VL-PAG administration of homo-AMPA increased the tail-flick latency and the paw withdrawal threshold in diabetic neuropathic mice. Homo-AMPA also reverted the enhancement of both, spontaneous and evoked activities of ON cells in diabetic neuropathic mice. In particular, homo-AMPA decreased the ongoing activity, the frequency of the burst and the duration of the burst of the ON cells.

4.3. The effect of homo-AMPA in the VL-PAG is not mediated through mGluR6 stimulation

Transcripts and proteins of the mGluR6 receptor were found in this study in the retinas of both, control and neuropathic diabetic mice, with a reduction in expression levels in diabetic mice, as already observed in diabetes conditions in the rat (Fan et al., 2020). However, despite the net effect of homo-AMPA on the nociceptive threshold and the activity of the ON and OFF neurons of RVM when microinjected into the VL PAG this study did not detect the presence of mGluR6 transcript and protein in the VL PAG, unlike other studies that found mGluR6 expression in brain areas such as cortex, hippocampus, olfactory bulb, the nucleus of solitary tract, superior colliculus, corpus callosum and subcommissural organ (Hoang and Hay, 2001; Young et al., 2008; Vardi et al., 2011; Dammann et al., 2018). In an attempt to identify the target by which homo-AMPA determined the effects on pain responses and the activity of the ON and OFF cells we conducted a pilot experiment in which homo-AMPA was administered in combination with MSOP, a group III antagonist of mGluRs. The MSOP was shown in this experiment to block the anti-allodynic effect of homo-AMPA. Based on this result and based on the fact that mGluR6 was not found in the VL PAG and that at the dose used homo-AMPA has no effect on mGluR4 and mGluR7, a possible target candidate for homo-AMPA it could be the mGluR8. Stimulation of mGluR8 at the level of the VL PAG, as in other areas such as the amygdala (Palazzo et al., 2008, 2011) and dorsal striatum (Rossi et al., 2014), has already been shown to inhibit pain responses and consistently modify the activity of the ON and OFF cells of the RVM (Marabese et al., 2007a,b; Hosseini et al., 2021). However, further studies are needed to confirm the activity of homo-AMPA on mGluR8, for example, the use of a mGluR8 selective antagonist or mGluR6 and/or mGluR8 knockout mice. It has been also reported that homo-AMPA, at higher doses than those used in the study (131 μM versus 30 μM) also acts as an N-methyl-D-aspartate (NMDA) receptor antagonist (Ahmadian et al., 1997). The possibility that homo-AMPA produced the observed effects through the NMDA receptor block is unlikely in this study: i) due to the homo-AMPA dose used (6 nmol corresponding to 30 μM) and ii) because NMDA receptor blockade at the level of the VL PAG would have inhibited (rather than stimulated) the activity of the descending pain modulatory pathway (Berrino et al., 2001; Palazzo et al., 2001, 2009). Among other things, the study underlines the need to carefully interpret the in vivo (and ex vivo) effects of homo-AMPA and to develop new ligands with greater selectivity towards mGluR6. The further necessary characterization of off-target actions of homo-AMPA will lead to a better understanding of the mechanisms underlying descending analgesia at the PAG level and new targets to address therapeutic strategies to relieve diabetic neuropathic pain. However, the potent analgesic effect of homo-AMPA in neuropathic pain conditions, whatever the target, deserves further consideration.

5. Conclusions

The current study is the first to evaluate the effect of homo-AMPA in diabetic neuropathy. Although the study did not show the presence of mGluR6 in the PAG-RVM pathway, the analgesic effect via the facilitation of the descending pathway is of great interest. It is thus evident that homo-AMPA acts in the brain on another target (mGluR8?), causing analgesia even at low concentrations. Overall, therefore, this study pushes us to re-evaluate the potential of this interesting molecule to understand its site of action and the possibility of therapeutic application in diabetic neuropathy.

Declaration of competing interest

None.

Acknowledgements

This work was supported by Ministero dell'Università e della Ricerca, MIUR, Research Projects of National Relevance, PRIN 2015, Prof. Sabatino Maione.

References

Ahmadian, H., Nielsen, B., Bräuner-Osborne, H., Johansen, T.N., Stensbøl, T.B., Sløk, F. A., Sekiyama, N., Nakanishi, S., Krogsgaard-Larsen, P., Madsen, U., 1997. (S)-homo-AMPA, a specific agonist at the mGlu6 subtype of metabotropic glutamic acid receptors. J. Med. Chem. 40, 3700–3705. https://doi.org/10.1021/jm9703597.

Bastyr 3rd, E.J., Price, K.L., Bril, V., MBBQ Study Group., 2005. Development and validity testing of the neuropathy total symptom score-6: questionnaire for the study of sensory symptoms of diabetic peripheral neuropathy. Clin. Therapeut. 27, 1278–1294. https://doi.org/10.1016/j.clinthera.2005.08.002.

Behbehani, M.M., Fields, H.L., 1979. Evidence that an excitatory connection between the periaqueductal gray and nucleus raphe magnus mediates stimulation produced analgesia. Brain Res. 170, 85–93. https://doi.org/10.1016/0006-8993(79)90942-9.

Berrino, L., Oliva, P., Rossi, F., Palazzo, E., Nobili, B., Maione, S., 2001. Interaction between metabotropic and NMDA glutamate receptors in the periaqueductal grey pain modulatory system. Naunyn-Schmiedeberg's Arch. Pharmacol. 364, 437–443. https://doi.org/10.1007/s002100100477.

Bräuner-Osborne, H., Sløk, F.A., Skjaerbaek, N., Ebert, B., Sekiyama, N., Nakanishi, S., Krogsgaard-Larsen, P., 1996. A new highly selective metabotropic excitatory amino acid agonist: 2-amino-4-(3-hydroxy-5-methylisoxazol-4-yl)butyric acid. J. Med. Chem. 39, 3188–3194. https://doi.org/10.1021/jm9602569.

Bräuner-Osborne, H., Egebjerg, J., Nielsen, E.O., Madsen, U., Krogsgaard-Larsen, P., 2000. Ligands for glutamate receptors: design and therapeutic prospects. J. Med. Chem. 43, 2609–2645. https://doi.org/10.1021/jm000007r.

Calcutt, N.A., Jorge, M.C., Yaksh, T.L., Chaplan, S.R., 1996. Tactile allodynia and formalin hyperalgesia in streptozotocin-diabetic rats: effects of insulin, aldose reductase inhibition and lidocaine. Pain 68, 293–299. https://doi.org/10.1016/s0304-3959(96)03201-0.

Dammann, F., Kirschstein, T., Guli, X., Müller, S., Porath, K., Rohde, M., Tokay, T., Köhling, R., 2018. Bidirectional shift of group III metabotropic glutamate receptor-mediated synaptic depression in the epileptic hippocampus. Epilepsy Res. 139, 157–163. https://doi.org/10.1016/j.eplepsyres.2017.12.002.

Devi, S., Markandeya, Y., Maddodi, N., Dhingra, A., Vardi, N., Balijepalli, R.C., Setaluri, V., 2013. Metabotropic glutamate receptor 6 signaling enhances TRPM1 calcium channel function and increases melanin content in human melanocytes. Pigm. Cell Melanoma Res. 26, 348–356. https://doi.org/10.1111/pcmr.12083.

Fan, Y., Lai, J., Yuan, Y., Wang, L., Wang, Q., Yuan, F., 2020. Taurine protects retinal cells and improves synaptic connections in early diabetic rats. Curr. Eye Res. 45, 52–63. https://doi.org/10.1080/02713683.2019.1653927.

Faden, A.I., Ivanova, S.A., Yakovlev, A.G., Mukhin, A.G., 1997. Neuroprotective effects of group III mGluR in traumatic neuronal injury. J. Neurotrauma 14, 885–895. https://doi.org/10.1089/neu.1997.14.885.

Fields, H.L., Bry, J., Hentall, I., 1983. The activity of neurons in the rostral medulla of the rat during withdrawal from noxious heat. J. Neurosci. 3, 2545–2552. https://doi.org/10.1523/JNEUROSCI.03-12-02545.1983.

Fields, H.L., Basbaum, A.I., 1999. Central nervous system mechanisms of pain modulation. In: Wall, P.D., Melzack, R. (Eds.), Textbook of Pain. London Churchill Livingstone, pp. 309–329.

Fields, H.L., Heinricher, M.M., Mason, P., 1991. Neurotransmitters in nociceptive modulatory circuits. Annu. Rev. Neurosci. 14, 219–245. https://doi.org/10.1146/annurev.ne.14.030191.001251.

Fields, H.L., Basbaum, A.I., Heinricher, M.M., 2005. Central nervous system mechanisms of pain modulation. In: McMahon, S.B., Koltzenburg, M. (Eds.), Textbook of Pain. Churchill Livingstone, Edinburgh, pp. 125–142.

Foreman, M.A., Gu, Y., Howl, J.D., Jones, S., Publicover, S.J., 2005. Group III metabotropic glutamate receptor activation inhibits Ca2+ influx and nitric oxide synthase activity in bone marrow stromal cells. J. Cell. Physiol. 204, 704–713. https://doi.org/10.1002/jcp.20353.

Gao, K., Mason, P., 2000. Serotonergic Raphe magnus cells that respond to noxious tail heat are not ON or OFF cells. J. Neurophysiol. 84, 1719–1725. https://doi.org/10.1152/jn.2000.84.4.1719.

Ghosh, P.K., Baskaran, N., van den Pol, A.N., 1997. Developmentally regulated gene expression of all eight metabotropic glutamate receptors in hypothalamic suprachiasmatic and arcuate nuclei–a PCR analysis. Brain Res. Dev. Brain Res. 102, 1–12. https://doi.org/10.1016/s0165-3806(97)00066-7.

Heinricher, M.M., Tavares, I., Leith, J.L., Lumb, B.M., 2009. Descending control of nociception: specificity, recruitment and plasticity. Brain Res. Rev. 60, 214–225. https://doi.org/10.1016/j.brainresrev.2008.12.009.

Hoang, C.J., Hay, M., 2001. Expression of metabotropic glutamate receptors in nodose ganglia and the nucleus of the solitary tract. Am. J. Physiol. Heart Circ. Physiol. 281, H457–H462. https://doi.org/10.1016/j.brainresrev.2008.12.009.

Hosseini, M., Parviz, M., Shabanzadeh, A.P., Zamani, E., 2021. Evaluation of the effect of (S)-3,4-Dicarboxyphenylglycine as a metabotropic glutamate receptors subtype 8 agonist on thermal nociception following central neuropathic pain. Asian Spine J. 15, 200–206. https://doi.org/10.31616/asj.2019.0367.

Jolivalt, C.G., Frizzi, K.E., Guernsey, L., Marquez, A., Ochoa, J., Rodriguez, M., Calcutt, N.A., 2017. Phenotyping peripheral neupathy in mouse models of diabetes. Curr. Protoc Mouse Biol. 6, 223–255. https://doi.org/10.1002/cpmo.11.

Khasabov, S.G., Brink, T.S., Schupp, M., Noack, J., Simone, D.A., 2012. Changes in response properties of rostral ventromedial medulla neurons during pro-longed inflammation: modulation by neurokinin-1 receptors. Neuroscience 224, 235–248. https://doi.org/10.1016/j.neuroscience.2012.08.029.

Koike, C., Obara, T., Uriu, Y., Numata, T., Sanuki, R., Miyata, K., Koyasu, T., Ueno, S., Funabiki, K., Tani, A., Ueda, H., Kondo, M., Mori, Y., Tachibana, M., Furukawa, T., 2010. TRPM1 is a component of the retinal ON bipolar cell transduction channel in the mGluR6 cascade. Proc. Natl. Acad. Sci. U.S.A. 107, 332–337. https://doi.org/10.1073/pnas.0912730107.

Lee-Kubli, C.A., Mixcoatl-Zecuatl, T., Jolivalt, C.G., Calcutt, N.A., 2014. Animal models of diabetes-induced neuropathic pain. Curr. Top Behav. Neurosci. 20, 147–170. https://doi.org/10.1007/7854_2014_280.

Leong, M.L., Gu, M., Speltz-Paiz, R., Stahura, E.I., Mottey, N., Steer, C.J., Wessendorf, M., 2011. Neuronal loss in the rostral ventromedial medulla in a rat model of neuropathic pain. J. Neurosci. 31, 17028–17039. https://doi.org/10.1523/JNEUROSCI.1268-11.2011.

Maione, S., Marabese, I., Leyva, J., Palazzo, E., de Novellis, V., Rossi, F., 1998. Characterisation of mGluRs which modulate nociception in the PAG of the mouse. Neuropharmacology 37, 1475–1483. https://doi.org/10.1016/s0028-3908(98)00126-9.

Maione, S., Oliva, P., Marabese, I., Palazzo, E., Rossi, F., Berrino, L., Filippelli, A., 2000. Periaqueductal gray matter metabotropic glutamate receptors modulate formalin-induced nociception. Pain 85, 183–189.

Marabese, I., Rossi, F., Palazzo, E., de Novellis, V., Starowicz, K., Cristino, L., Vita, D., Gatta, L., Guida, F., Di Marzo, V., Rossi, F., Maione, S., 2007a. Periaqueductal gray metabotropic glutamate receptor subtype 7 and 8 mediate opposite effects on amino acid release, rostral ventromedial medulla cell activities, and thermal nociception. J. Neurophysiol. 98, 43–53. https://doi.org/10.1152/jn.00356.2007.

Marabese, I., de Novellis, V., Palazzo, E., Scafuro, M.A., Vita, D., Rossi, F., Maione, S., 2007b. Effects of (S)-3,4-DCPG, an mGlu8 receptor agonist, on inflammatory and neuropathic pain in mice. Neuropharmacology 52, 253–262.

Marciniak, M., Chruścicka, B., Lech, T., Burnat, G., Pilc, A., 2016. Expression of group III metabotropic glutamate receptors in the reproductive system of male mice. Reprod. Fertil. Dev. 28, 369–374. https://doi.org/10.1071/RD14132.

Millan, M.J., 2002. Descending control of pain. Prog. Neurobiol. 66, 355–474. https://doi.org/10.1016/s0301-0082(02)00009-6.

Moreau, J.L., Fields, H.L., 1986. Evidence for GABA involvement in midbrain control of medullary neurons that modulate nociceptive transmission. Brain Res. 397, 37–46. https://doi.org/10.1016/0006-8993(86)91367-3.

Morgado, C., Pinto-Ribeiro, F., Tavares, I., 2008. Diabetes affects the expression of GABA and potassium chloride cotransporter in the spinal cord: a study instreptozotocin diabetic rats. Neurosci. Lett. 438, 102–106. https://doi.org/10.1016/j.neulet.2008.04.032.

Morgans, C.W., Zhang, J., Jeffrey, B.G., Nelson, S.M., Burke, N.S., Duvoisin, R.M., Brown, R.L., 2009. TRPM1 is required for the depolarizing light response in retinal ON-bipolar cells. Proc. Natl. Acad. Sci. U. S. A. 106, 19174–19178. https://doi.org/10.1073/pnas.0908711106.

Morrow, T.J., 2004. Animal models of painful diabetic neuropathy: the STZ rat model. Curr. Protoc. Neurosci. 9, 9–18. https://doi.org/10.1002/0471142301.ns0918s29.

Nakajima, Y., Iwakabe, H., Akazawa, C., Nawa, H., Shigemoto, R., Mizuno, N., Nakanishi, S., 1993. Molecular characterization of a novel retinal Metabotropic glutamate receptor mGluR6 with a high agonist selectivity for L-2-amino-4-phosphonobutyrate. J. Biol. Chem. 268, 11868–11873.

Nawy, S., Jahr, C.E., 1990. Suppression by glutamate of cGMP-activated conductance in retina bipolar cells. Nature 346, 269–271. https://doi.org/10.1038/346269a0.

O'Brien, D.E., Conn, P.J., 2016. Neurobiological insights from mGlu receptor allosteric modulation. Int. J. Neuropsychopharmacol. 19, pyv133. https://doi.org/10.1093/ijnp/pyv133.

Ossipov, M.H., Dussor, G.O., Porreca, F., 2010. Central modulation of pain. J. Clin. Invest. 120, 3779–3787. https://doi.org/10.1172/JCI43766.

Palazzo, E., Marabese, I., de Novellis, V., Oliva, P., Rossi, F., Berrino, L., Rossi, F., Maione, S., 2001. Metabotropic and NMDA glutamate receptors participate in the cannabinoid-induced antinociception. Neuropharmacology 40, 319–326. https://doi.org/10.1016/s0028-3908(00)00160-x.

Palazzo, E., Fu, Y., Ji, G., Maione, S., Neugebauer, V., 2008. Group III mGluR7 and mGluR8 in the amygdala differentially modulate nocifensive and affective pain behaviors. Neuropharmacology 55, 537–545. https://doi.org/10.1016/j.neuropharm.2008.05.007.

Palazzo, E., Guida, F., Migliozzi, A., Gatta, L., Marabese, I., Luongo, L., Rossi, C., de Novellis, V., Fernández-Sánchez, E., Soukupova, M., Zafra, F., Maione, S., 2009. Intraperiaqueductal gray glycine and D-serine exert dual effects on rostral ventromedial medulla ON- and OFF-cell activity and thermoceptive threshold in the rat. J. Neurophysiol. 102, 3169–3179. https://doi.org/10.1152/jn.00124.2009.

Palazzo, E., Marabese, I., Soukupova, M., Luongo, L., Boccella, S., Giordano, C., de Novellis, V., Rossi, F., Maione, S., 2011. Metabotropic glutamate receptor subtype 8 in the amygdala modulates thermal threshold, neurotransmitter release, and rostral ventromedial medulla cell activity in inflammatory pain. J. Neurosci. 31, 4687–4697. https://doi.org/10.1523/JNEUROSCI.2938-10.2011.

Palazzo, E., Marabese, I., Luongo, L., Boccella, S., Bellini, G., Giordano, M.E., Rossi, F., Scafuro, M., de Novellis, V., Maione, S., 2013. Effects of a metabotropic glutamate receptor subtype 7 negative allosteric modulator in the periaqueductal grey on pain responses and rostral ventromedial medulla cell activity in rat. Mol. Pain 9, 44. https://doi.org/10.1186/1744-8069-9-44.

Palazzo, E., Romano, R., Luongo, L., Boccella, S., De Gregorio, D., Giordano, M.E., Rossi, F., Marabese, I., Scafuro, M.A., de Novellis, V., Maione, S., 2015. MMPIP, an mGluR7-selective negative allosteric modulator, alleviates pain and normalizes

affective and cognitive behavior in neuropathic mice. Pain 156, 1060–1073. https://doi.org/10.1097/j.pain.0000000000000150.

Palazzo, E., Boccella, S., Marabese, I., Pierretti, G., Guida, F., Maione, S., 2020. The cold case of metabotropic glutamate receptor 6: unjust detention in the retina? Curr. Neuropharmacol. 18, 120–125. https://doi.org/10.2174/1570159X17666191001141849.

Pałucha, A., Tatarczyńska, E., Brański, P., Szewczyk, B., Wierońska, J.M., Kłak, K., Chojnacka-Wójcik, E., Nowak, G., Pilc, A., 2004. Group III mGlu receptor agonists produce anxiolytic- and antidepressant-like effects after central administration in rats. Neuropharmacology 46, 151–159.

Paxinos, G., Franklin, K., 1997. Paxinos and Franklin's the Mouse Brain in Stereotaxic Coordinates, fourth ed. Academic Press, San Diego, CA, USA. https://doi.org/10.1016/j.neuropharm.2003.09.006.

Pissimissis, N., Papageorgiou, E., Lembessis, P., Armakolas, A., Koutsilieris, M., 2009. The glutamatergic system expression in human PC-3 and LNCaP prostate cancer cells. Anticancer Res. 29, 371–377.

Prieto, G.J., Cannon, J.T., Liebeskind, J.C., 1983. N. raphe magnus lesions disrupt stimulation-produced analgesia from ventral but not dorsal midbrain areas in the rat. Brain Res. 261, 53–57. https://doi.org/10.1016/0006-8993(83)91282-9.

Rossi, F., Marabese, I., De Chiaro, M., Boccella, S., Luongo, L., Guida, F., De Gregorio, D., Giordano, C., de Novellis, V., Palazzo, E., Maione, S., 2014. Dorsal striatum metabotropic glutamate receptor 8 affects nocifensive responses and rostral ventromedial medulla cell activity in neuropathic pain conditions. J. Neurophysiol. 111, 2196–2209. https://doi.org/10.1152/jn.00212.2013.

Salas, R., Ramirez, K., Vanegas, H., Vazquez, E., 2016. Activity correlations between on-like and off-like cells of the rostral ventromedial medulla and simultaneously recorded wide-dynamic-range neurons of the spinal dorsal horn in rats. Brain Res. 1652, 103–110. https://doi.org/10.1016/j.brainres.2016.10.001.

Sandkühler, J., Gebhart, G.F., 1984. Relative contributions of the nucleus raphe magnus and adjacent medullary reticular formation to the inhibition by stimulation in the periaqueductal gray of a spinal nociceptive reflex in the pentobarbital-anesthetized rat. Brain Res. 305, 77–87. https://doi.org/10.1016/0006-8993(84)91121-1.

Schoepp, D.D., Jane, D.E., Monn, J.A., 1999. Pharmacological agents acting at subtypes of metabotropic glutamate receptors. Neuropharmacology 38, 1431–1476. https://doi.org/10.1016/s0028-3908(99)00092-1.

Silva, M., Amorim, D., Almeida, A., Tavares, I., Pinto-Ribeiro, F., Morgado, C., 2013. Pronociceptive changes in the activity of rostroventromedial medulla (RVM) pain modulatory cells in the streptozotocin-diabetic rat. Brain Res. Bull. 96, 39–44. https://doi.org/10.1016/j.brainresbull.2013.04.008.

Taylor, D.L., Diemel, L.T., Pocock, J.M., 2003. Activation of microglial group III metabotropic glutamate receptors protects neurons against microglial neurotoxicity. J. Neurosci. 23, 2150–2160. https://doi.org/10.1523/JNEUROSCI.23-06-02150.2003.

Thomas, N.K., Jane, D.E., Tse, H.W., Watkins, J.C., 1996. Alpha-Methyl derivatives of serine-O-phosphate as novel, selective competitive metabotropic glutamate receptor antagonists. Neuropharmacology 35, 637–642. https://doi.org/10.1016/0028-3908(96)84635-1.

Vanegas, H., Schaible, H.G., 2004. Descending control of persistent pain: inhibitoryorfacilitatory? Brain Res. Rev. 46, 295–309. https://doi.org/10.1016/j.brainresrev.2004.07.004.

Vardi, T., Fina, M., Zhang, L., Dhingra, A., Vardi, N., 2011. mGluR6 transcripts in non-neuronal tissues. J. Histochem. Cytochem. 59, 1076–1086. https://doi.org/10.1369/0022155411425386.

Vilar, B., Busserolles, J., Ling, B., Laffray, S., Ulmann, L., Malhaire, F., Chapuy, E., Aissouni, Y., Etienne, M., Bourinet, E., Acher, F., Pin, J.P., Eschalier, A., Goudet, C., 2013. Alleviating pain hypersensitivity through activation of type 4 metabotropic glutamate receptor. J. Neurosci. 33, 18951–18965. https://doi.org/10.1523/JNEUROSCI.1221-13.2013.

Vinik, A.I., Milicevic, Z., Pittenger, G.L., 1995. Beyond glycemia. Diabetes Care 18, 1037–1041. https://doi.org/10.2337/diacare.18.7.1037.

Wang, H., Jiang, W., Yang, R., Li, Y., 2011. Spinal metabotropic glutamate receptor 4 is involved in neuropathic pain. Neuroreport 22, 244–248. https://doi.org/10.1097/WNR.0b013e3283453843.

Young, R.L., Cooper, N.J., Blackshaw, L.A., 2008. Anatomy and function of group III metabotropic glutamate receptors in gastric vagal pathways. Neuropharmacology 54, 965–975.

Zheng, S., Sun, Z., Ni, J., Li, Z., Sha, Y., Zhang, T., Qiao, S., Zhao, G., Song, Z., 2016. mGluR6 regulates keratinocyte phagocytosis by modulating CaM KII/ERK/MLC signalling pathway. Exp. Dermatol. 25, 909–911.